New treatment of breakup continuum in the method of continuum discretized coupled channels

T. Matsumoto,[1,*] T. Kamizato,[2] K. Ogata,[1] Y. Iseri,[3] E. Hiyama,[4] M. Kamimura,[1] and M. Yahiro[2]
[1]*Department of Physics, Kyushu University, Fukuoka 812-8581, Japan*
[2]*Department of Physics and Earth Sciences, University of the Ryukyus, Nishihara-cho, Okinawa 903-0213, Japan*
[3]*Department of Physics, Chiba-Keizai College, Todoroki-cho 4-3-30, Inage, Chiba 263-0021, Japan*
[4]*Institute of Particle and Nuclear Studies, High Energy Accelerator Research Organization (KEK), Tsukuba 305-0801, Japan*
(Received 10 February 2003; published 16 December 2003)

A new method of pseudostate discretization is proposed for the method of continuum discretized coupled channels to deal with three-body breakup processes. In the method, discrete *S*-matrix elements to the pseudo (discretized) continuum states are transformed into smooth ones to the exact continuum states of the projectile. As for the basis functions for describing pseudostate wave functions, we take real- and complex-range Gaussian functions, which form in good approximation a complete set in a finite configuration space being important for breakup processes. This "approximate-completeness" property is essential to make transformed *S*-matrix elements accurate. Moreover, the use of these Gaussian bases is expected to be very useful to describe four-body breakup processes. Accuracy of the method is tested quantitatively for two realistic examples: elastic and projectile-breakup processes in $d+^{58}$Ni scattering at 80 MeV and those in ^{6}Li$+^{40}$Ca at 156 MeV.

DOI: 10.1103/PhysRevC.68.064607 PACS number(s): 24.10.Eq, 25.45.De, 25.60.Gc, 25.70.Ef

I. INTRODUCTION

The method of continuum discretized coupled channels (CDCC) has been successful in describing nuclear reactions including weakly bound projectiles [1–12]. CDCC has been attracting much attention since the advent of experiments with radioactive beams, because projectile breakup processes are essential to many of such reactions [11,12]. CDCC plays an important role in the spectroscopic studies of radioactive nuclei through the nuclear reactions involving such nuclei.

In CDCC for reactions with a projectile consisting of two fragments, the states of the projectile are classified by the linear and the angular momenta, k and ℓ, of relative motion of the two fragments of the projectile, which are truncated by $k \leqslant k_{\max}$ and $\ell \leqslant \ell_{\max}$. The truncation is the most basic assumption in CDCC, and it is confirmed that calculated *S*-matrix elements converge for sufficiently large $k_{\max}$ and $\ell_{\max}$ [1,3,13]. It has been shown that CDCC is the first-order approximation to the distorted Faddeev equations, and corrections to the converged CDCC solution are negligible within the region of space in which the reaction takes place [14].

As a consequence of the truncation, the integral equation form of the equations of coupled channels, derived from the three-body Schrödinger equation, has a compact kernel, indicating that the equation is soluble mathematically [14]. In practice, however, the coupled channels equations thus obtained are impossible to be solved because of the continuously infinite number of coupled breakup channels. The problem is solved by discretizing the k continuum. The discretization leads the coupled equations to a set of differential equations with a finite number of channels.

As for the discretization, two kinds of methods have been proposed so far, i.e., the momentum-bin method [1–3,13,15] and the pseudostate (PS) method [1,16,17]. In the momentum-bin method, which consists of the average (Av) [1–3,15] and the midpoint (Mid) [2,13] methods, the k-continuum is divided into a finite number of bins. The continuum channels within each bin state are then represented by a single channel; the averaged state over k in the Av method and the state at the midpoint of the bin in the Mid method. It has been confirmed that calculated *S*-matrix elements converge as the width Δ of the bins is decreased, and also that the two methods yield the same converged *S*-matrix elements [1,3,13]. From a practical point of view, the Av method requires less numerical works than the Mid one [13]; the Av method therefore is most widely used. In the PS method, on the other hand, wave functions of the discretized breakup states are obtained by diagonalizing the internal Hamiltonian of the projectile, which describes the relative motion of the two constituents, using L^2-type basis functions. Since the wave functions of such pseudobreakup states have wrong asymptotic forms, the PS method was mainly used in the past to describe virtual breakup processes in the intermediate stage of elastic scattering [17] and (d,p) reactions [1].

Independent of the choice of the discretization methods, one obtains as a result of CDCC calculation discrete *S*-matrix elements to the discretized breakup states, say $\{S_i;\ i=0-N\}$, as illustrated in Fig. 1(a); S_i is given as a spike-type function with respect to k. In the momentum-bin method, "breakup *S*-matrix elements" $S(k)$, which describes the transition to the k-continuum, are then approximately constructed by the histogram with the width Δ as illustrated in Fig. 1(b); $S(k)$ satisfies the condition that S_i equals to the integration of $S(k)$ over k within the region corresponding to the ith bin. An explicit formula to derive $S(k)$ from $\{S_i\}$ was given by Eq. (9) in Ref. [18], where the derived $S(k)$ is continuous within each bin but not in the entire range of k, just the same as in Fig. 1(b). A prescription to derive $S(k)$ from $\{S_i\}$ within the PS method was recently proposed in Ref. [16] by assuming a histogram form of $S(k)$ with different magnitudes of widths,

*Electronic address: taku2scp@mbox.nc.kyushu-u.ac.jp

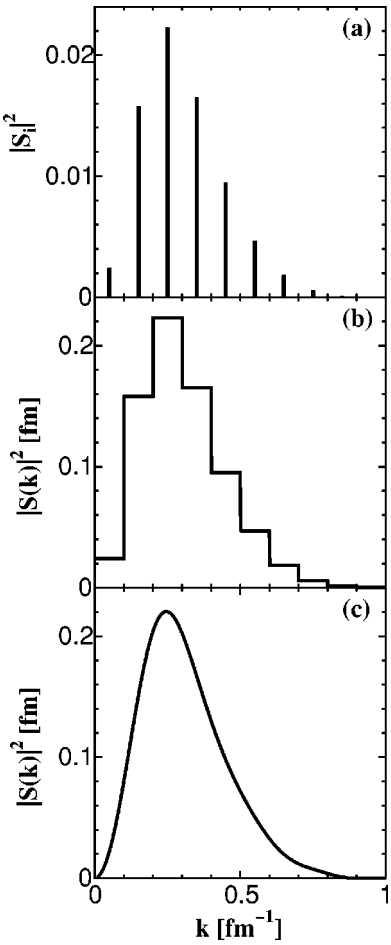

FIG. 1. Schematic illustration of three types of *S*-matrix elements for breakup continuum states. See text.

which were estimated in a reasonable way. The resultant $S(k)$ was found to be similar to that obtained by the momentum-bin method.

Thus, so far breakup *S*-matrix elements $S(k)$ obtained by CDCC have a form such as that in Fig. 1(b), namely, not smooth in the entire range of k. However, in the CDCC calculation of coincidence cross sections of the projectile fragments, such as (d,pn) [4], it is desirable to transform the histogram function $S(k)$ [Fig. 1(b)] into a smooth function of k, such as in Fig. 1(c). In the calculations in Ref. [4], a smooth $S(k)$ was obtained by simply interpolating the histogram using polynomial functions of k, the accuracy of which needs be examined.

The purpose of the present paper is to propose a new PS method for projectile-breakup reactions, which generates accurate breakup *S*-matrix elements as a smooth function of k in its entire range. In order to achieve this purpose, we employ appropriate basis functions in the PS method and apply them to the "smoothing procedure" of Ref. [18] that is based on the Av method. The new method assumes no form *a priori* for k distributions of breakup *S*-matrix elements $S(k)$, same as in Ref. [18], and is independent of the type of the basis functions used for the PS method. The only condition for the basis functions for the PS wave functions is that they constitute an approximate complete set in the wide range of

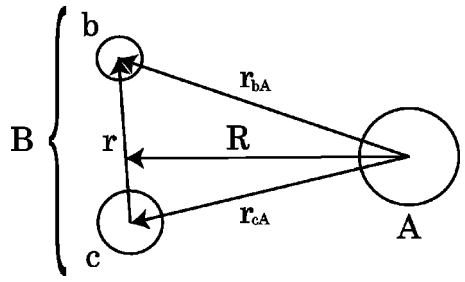

FIG. 2. Illustration of a three-body $(A+b+c)$ system. The symbol $B=b+c$ stands for the projectile, and A is the target.

k and its conjugate coordinate r which are important for the breakup processes. As basis functions which satisfy this condition, we propose to employ the following two bases. One is a set of ordinary Gaussian functions [19], which we refer to as *real-range Gaussian functions* in the present paper. The other is a natural extension of that, *complex-range Gaussian functions* [20], i.e., Gaussian functions with the complex range parameters, the precise definition of which is given later. With these basis functions it is verified that $S(k)$ of a smooth function obtained by the new PS method is consistent with the histogram-type $S(k)$ obtained by the Av method with a very small width Δ. It should be noted that the use of these bases of Gaussian form is extremely important for the simplification of numerical calculations, even in a case where projectile is assumed to be composed of *three* particles; cf. Ref. [20] on the Gaussian expansion method for few-body systems.

In Sec. II, we recapitulate CDCC based on both the Av and the PS methods of discretization. In Sec. III, we describe a method of interpolation to obtain continuous breakup *S*-matrix elements from discrete ones calculated with the PS method, and introduce the real- and the complex-range Gaussian basis. In Sec. IV, the validity of the present PS method is tested and justified for two realistic cases, $d+{}^{58}$Ni scattering at 80 MeV and ^{6}Li$+{}^{40}$Ca scattering at 156 MeV. In Sec. V, discussion is made for the potentiality of the present PS method for four-body breakup reactions in which the projectile is assumed to be composed of three particles. Section VI gives a summary.

II. THE METHOD OF CONTINUUM DISCRETIZED COUPLED CHANNELS

We consider a reaction of a weakly bound projectile B impinging on a target nucleus A. We treat a simple system shown in Fig. 2 in which the projectile B is composed of two particles b and c and the target A is inert. The three-body system is described by a model Hamiltonian

$$H = H_{\rm bc} + K_R + U_{\rm Coul}(R) + U,$$

$$H_{\rm bc} = K_r + V_{\rm bc}(\mathbf{r}),$$

$$U = U_{\rm bA}(\mathbf{r}_{\rm bA}) + U_{\rm cA}(\mathbf{r}_{\rm cA}). \qquad (1)$$

Vector $\mathbf{r}$ is the relative coordinate between b and c, $\mathbf{R}$ the one between the center of mass of the b-c pair and A, and $\mathbf{r}_{\rm XY}$

denotes the relative coordinate between two particles X and Y. Operators K_r and K_R are kinetic energies associated with $\mathbf{r}$ and $\mathbf{R}$, respectively, and $V_{\rm bc}(\mathbf{r})$ is the interaction between b and c. The interaction $U_{\rm bA}(U_{\rm cA})$ between $b(c)$ and A is taken to be the optical potential for $b+A(c+A)$ scattering. For simplicity, the spin dependence of the interactions is neglected. Furthermore, the Coulomb potential between A and B is treated approximately as a function only of R, i.e., we neglect Coulomb breakup processes and focus our attention on nuclear breakup.

In CDCC, the three-body wave function Ψ_{JM}, with the total angular momentum J and its projection M on z axis, is expanded in terms of the orthonormal set of eigenstates Φ of $H_{\rm bc}$:

$$\Psi_{JM}(\mathbf{r},\mathbf{R}) = \sum_L \mathcal{Y}^{\ell_0,L}_{JM}\Phi_0(r)\chi_{\ell_0 LJ}(P_0,R)/R + \sum_{\ell,L}\mathcal{Y}^{\ell,L}_{JM}\int_0^\infty \Phi_\ell(k,r)\chi_{\ell LJ}(P,R)/R\, dk, \quad (2)$$

where

$$\mathcal{Y}^{\ell,L}_{JM} = [i^\ell Y_\ell(\Omega_r)\otimes i^L Y_L(\Omega_R)]_{JM}. \quad (3)$$

For simplicity, we assume that the $b+c$ system has one bound state $\Phi_0(r)$ with angular momentum ℓ_0 and continuum states $\Phi_\ell(k,r)$ with linear momentum k and angular momentum ℓ, both ranging from zero to infinity. The $\Phi_\ell(k,r)$ are real functions normalized to the δ function in k [3]. The projectile B is initially in the bound state. The coefficient $\chi_{\ell LJ}(\chi_{\ell_0 LJ})$ of the expansion describes center-of-mass motion of the b-c pair relative to A in the state Φ_ℓ (Φ_0) with the linear and orbital angular momenta P (P_0) and L, respectively.

In CDCC, the sum over ℓ is truncated by $\ell\leqslant\ell_{\rm max}$ and the k integral by $k\leqslant k_{\rm max}$. For each ℓ, furthermore, the continuum states from $k=0$ to $k_{\rm max}$ are discretized into a finite number of states. The orthonormalized wave functions are denoted by $\{\hat\Phi_{i\ell}(r)i^\ell Y_{\ell m}(\Omega_r); i=1-N\}$ whose energies $\epsilon_{i\ell}$ are given by

$$\epsilon_{i\ell}\delta_{i,i'} = \langle\hat\Phi_{i\ell}(r)i^\ell Y_{\ell m}(\Omega_r)|H_{\rm bc}|\hat\Phi_{i'\ell}(r)i^\ell Y_{\ell m}(\Omega_r)\rangle_{\mathbf{r}}. \quad (4)$$

Details of the discretization are described in the following section.

After the truncation and the discretization, Ψ_{JM} is reduced to an approximate one,

$$\Psi^{\rm CDCC}_{JM} = \sum_L \mathcal{Y}^{\ell_0,L}_{JM}\Phi_0(r)\hat\chi_{\gamma_0}(P_0,R)/R + \sum_{l=0}^{l_{\rm max}}\sum_{i=1}^{N}\sum_L \mathcal{Y}^{\ell,L}_{JM}\hat\Phi_{i\ell}(r)\hat\chi_\gamma(\hat P_\gamma,R)/R, \quad (5)$$

where

$$\hat\chi_{\gamma_0}(P_0,R) = \chi_{\gamma_0}(P_0,R),\ \gamma_0=(0,\ell_0,L,J),$$
$$\hat\chi_\gamma(\hat P_\gamma,R) = W_\gamma\chi_\gamma(\hat P_\gamma,R),\ \gamma=(i,\ell,L,J).$$

On the right hand side of Eq. (5), the first term represents the elastic channel denoted by γ_0 and the second one corresponds to the discretized breakup channels, each denoted by γ. The weight factor W_γ depends on the discretization method used. The momenta P_0 and $\hat P_\gamma$ satisfy the total energy conservation:

$$E = \hbar^2P_0^2/2\mu_{\rm AB} + \epsilon_0 = \hbar^2\hat P_\gamma^2/2\mu_{\rm AB} + \epsilon_{i\ell}, \quad (6)$$

where $\mu_{\rm AB}$ is the reduced mass of the A-B system and ϵ_0 $(\epsilon_{i\ell})$ is the energy of B in the ground (discretized continuum) state.

Inserting Eq. (5) into the approximate three-body Schrödinger equation $(H-E)\Psi^{\rm CDCC}_{JM}=0$ leads to a set of coupled differential equations for $\hat\chi_{\gamma_0}(P_0,R)$ and $\hat\chi_\gamma(\hat P_i,R)$:

$$\left[\frac{d^2}{dR^2} + \hat P_\gamma^2 - \frac{L(L+1)}{R^2} - \frac{2\mu_{\rm AB}}{\hbar^2}V_{\gamma\gamma}(R)\right]\hat\chi_\gamma(\hat P_\gamma,R) = \sum_{\gamma'\neq\gamma}\frac{2\mu_{\rm AB}}{\hbar^2}V_{\gamma\gamma'}(R)\hat\chi_{\gamma'}(\hat P_{\gamma'},R) \quad (7)$$

for all γ including γ_0, where $\hat P_0=P_0$. The coupling potentials $V_{\gamma\gamma'}(R)$ are obtained by

$$V_{\gamma\gamma'}(R) = \langle\mathcal{Y}^{\ell,L}_{JM}\hat\Phi_{i\ell}(r)|U|\mathcal{Y}^{\ell',L'}_{JM}\hat\Phi_{i'\ell'}(r)\rangle_{\mathbf{r},\Omega_R}. \quad (8)$$

The coupled equations are solved under the asymptotic boundary condition

$$\hat\chi_\gamma(\hat P_\gamma,R) \sim u_L^{(-)}(\hat P_\gamma,R)\delta_{\gamma,\gamma_0} - \sqrt{\frac{\hat P_\gamma}{\hat P_0}}\hat S_{\gamma,\gamma_0}u_L^{(+)}(\hat P_\gamma,R). \quad (9)$$

Here $u_L^{(-)}(\hat P_\gamma,R)$ and $u_L^{(+)}(\hat P_\gamma,R)$ are incoming and outgoing Coulomb wave functions with the momentum $\hat P_\gamma$. The quantity $\hat S_{\gamma,\gamma_0}$ is the discrete S-matrix element for the transition from the initial channel γ_0 to a discretized continuum one γ [cf. Fig. 1(a)].

III. DISCRETIZATION OF k CONTINUUM

Among the three methods of discretization of the k continuum, the relation between the Av and the Mid methods has already been clarified [13]. The present discussion therefore is focused on the Av and the PS methods.

A. The average method

In the Av method, the k-continuum $[0,k_{\rm max}]$, for each ℓ, is divided into a finite number of bins, each with a width $\Delta_{i\ell}=k_i-k_{i-1}$, and the continuum breakup states in the ith bin are averaged with a weight function $f_{i\ell}(k)$ [1,2]. The resultant orthonormal state is described as

$$\hat\Phi_{i\ell}(r) = \frac{1}{W_\gamma}\int_{k_{i-1}}^{k_i}\Phi_\ell(k,r)f_{i\ell}(k)dk \quad \text{(for Av)}, \quad (10)$$

then the weight factor W_γ is given by

$$W_\gamma^2 = \int_{k_{i-1}}^{k_i} [f_{i\ell}(k)]^2 \, dk. \tag{11}$$

For a bin far from a resonance, it is natural to set $f_{i\ell}(k) = 1$, so that $W_\gamma = \sqrt{\Delta_{i\ell}}$, since $\Phi_\ell(k, r)$ changes smoothly with k. On the other hand, $\Phi_\ell(k, r)$ changes rapidly across the resonance. One way of coping with this situation is to take $\Delta_{i\ell}$ much smaller than the width of the resonance so that $\Phi_\ell(k, r)$ does not change much within individual bins. This, however, makes the number of bins large. Alternatively, one can take a single bin which contains the whole resonance peak and use a weight function of Breit-Wigner type [1,5,6,8,10],

$$f_{i\ell}(k) = \left| \frac{i\Gamma/2}{\epsilon(k) - \epsilon_{\rm res} + i\Gamma/2} \right|, \tag{12}$$

where $\epsilon(k)$ is a continuous intrinsic energy of the $b+c$ system. The discretized intrinsic energy $\epsilon_i = \hbar^2 \hat{k}_i^2 / 2\mu_{\rm bc}$ corresponding to each bin is obtained as $\hat{k}_i^2 = (k_i + k_{i-1})^2/4 + \Delta_{i\ell}^2/12$ for a nonresonance bin and $\epsilon_i = \epsilon_{\rm res}$ for a resonance one.

Comparing the approximate form (5) with the exact one (2) in the asymptotic region $R \to \infty$, it is natural to assume

$$S_{\ell,L}^{(J)}(k) = \frac{\hat{S}_{\gamma,\gamma_0}}{W_\gamma} f_{i\ell}(k) \quad \text{for } k_{i-1} < k \leqslant k_i \tag{13}$$

to hold in a good approximation, which was confirmed by Tostevin *et al.* [18] in the framework of the Av method. They employed, in actual calculation, $f_{i\ell}(k) = 1$ for $\ell > 0$ as described above, while $f_{i\ell}(k) \propto k$ for $\ell = 0$, which gives a change of W_γ, i.e., $W_\gamma \propto (k_i^3 - k_{i-1}^3)^{1/2}$. In any case, it should be noted that $S_{\ell,L}^{(J)}(k)$ given by Eq. (13) is continuous only within each k-bin region but not in the entire k [cf. Fig. 1(b)].

B. The pseudostate method

In the PS method, we diagonalize $H_{\rm bc}$ in a space spanned by a finite number of L^2-type basis functions, say $\{\phi_{j\ell}(r)\}$, and obtain discrete eigenstates $\{\hat{\Phi}_{i\ell}(r)\}$ as

$$\hat{\Phi}_{i\ell}(r) = \sum_j A_{i\ell,j} \, \phi_{j\ell}(r). \tag{14}$$

The k continuum is automatically discretized by identifying the ith eigenstates above the breakup threshold with $\hat{\Phi}_{i\ell}(r)$. The weight factor W_γ is unity if the resultant discretized states $\hat{\Phi}_{i\ell}(r)$ are orthonormalized. Among the eigenstates, only low-lying states belonging to the region $0 < \epsilon \leqslant \hbar^2 k_{\rm cut}^2 / 2\mu_{\rm bc}$ are taken as breakup channels in CDCC equation (7), where $k_{\rm cut}$ is the cutoff value of k corresponding to $k_{\rm max}$ in the Av method.

The CDCC equations (7) thus obtained yield discrete breakup S-matrix elements. If the basis functions form a complete set with good accuracy in the region of r and k being important for breakup processes, an accurate transformation from the discrete S-matrix elements to the continuous ("exact") ones is possible, applying the prescription given in Ref. [18] to the PS method as follows. The exact breakup T-matrix element is given by

$$T_{\ell L}^{(J)}(k) = \langle \Phi_\ell(k, r) u_L^{(-)}(P, R) Y_{JM}^{\ell,L} | U | \Psi_{JM} \rangle. \tag{15}$$

Inserting the approximate complete set $\{\hat{\Phi}_{i\ell}(r)\}$ between the bra vector and the operator U in Eq. (15), and replacing the ket vector by the CDCC wave function (5), one obtains the following approximate relation:

$$\begin{aligned} T_{\ell L}^{(J)}(k) &\approx \sum_i f_{i\ell}^{\rm PS}(k) \langle \hat{\Phi}_{i\ell}(r) u_L^{(-)}(P, R) \mathcal{Y}_{JM}^{\ell,L} | U | \Psi_{JM}^{\rm CDCC} \rangle \\ &\approx \sum_i f_{i\ell}^{\rm PS}(k) \hat{T}_{\gamma,\gamma_0}, \end{aligned} \tag{16}$$

where

$$f_{i\ell}^{\rm PS}(k) = \langle \Phi_\ell(k, r) | \hat{\Phi}_{i\ell}(r) \rangle \tag{17}$$

and

$$\hat{T}_{\gamma,\gamma_0} = \langle \hat{\Phi}_{i\ell} u_L^{(-)}(\hat{P}_\gamma, R) \mathcal{Y}_{JM}^{\ell,L} | U | \Psi_{JM}^{\rm CDCC} \rangle. \tag{18}$$

The last form of Eq. (16) has been derived by replacing P by $\hat{P}_\gamma$ in $u_L^{(-)}(P, R)$, which is valid since the k distribution of $f_{i\ell}^{\rm PS}(k)$ is sharply localized at $k = \hat{k}_i = \sqrt{2\mu_{\rm bc}\epsilon_{i\ell}}/\hbar$. $\hat{T}_{\gamma,\gamma_0}$ is a CDCC breakup T-matrix element calculated with CDCC. Since the $\hat{T}_{\gamma,\gamma_0}$ are proportional to the corresponding S-matrix elements $\hat{S}_{\gamma,\gamma_0}$,

$$S_{\ell L}^{(J)}(k) \approx \sum_i f_{i\ell}^{\rm PS}(k) \hat{S}_{\gamma,\gamma_0}. \tag{19}$$

The "k-interpolation formula" (19) for the PS method agrees with the corresponding one in Ref. [18] for the Av method. Thus, Eq. (19) can be used for any method of discretization, if the discretized wave functions constitute an approximate complete set. The interpolation formula is also independent of the type of the basis function taken, as obvious from the derivation.

As such basis functions, we here propose two types; one is the conventional real-range Gaussian functions

$$\phi_{j\ell}(r) = r^\ell \exp[-(r/a_j)^2] \quad (j = 1 - n), \tag{20}$$

where $\{a_j\}$ are assumed to increase in a geometric progression [19]:

$$a_j = a_1 (a_n / a_1)^{(j-1)/(n-1)}. \tag{21}$$

The other is an extension of Eq. (20) introduced in Ref. [20], i.e., the following pairs of functions:

TABLE I. Parameters of the optical potentials for $n+^{58}$Ni and $p+^{58}$Ni at half the deuteron incident energy. We followed the same notation as in Ref. [21].

System	V_0 (MeV)	r_0 (fm)	a_0 (fm)	W_0 (MeV)	r_W (fm)	a_W (fm)	W_D (MeV)	r_{WD} (fm)	a_{WD} (fm)
$p+^{58}$Ni	44.921	1.17	0.750	6.10	1.32	0.534	2.214	1.32	0.534
$n+^{58}$Ni	42.672	1.17	0.750	7.24	1.26	0.580	2.586	1.26	0.580

$$\phi^{\mathrm{C}}_{j\ell}(r) = r^{\ell}\exp[-(r/a_j)^2]\cos[b(r/a_j)^2],$$

$$\phi^{\mathrm{S}}_{j\ell}(r) = r^{\ell}\exp[-(r/a_j)^2]\sin[b(r/a_j)^2] \quad (j = 1-n). \quad (22)$$

Here, b is a free parameter, in principle, but numerical test showed that $b=\pi/2$ is recommendable. Both $\phi^{\mathrm{C}}_{j\ell}$ and $\phi^{\mathrm{S}}_{j\ell}$ are used as the basis functions $\phi_{j\ell}$ in Eq. (14); the total number of basis is thus $2n$.

The basis functions (22) can also be expressed as

$$\phi^{\mathrm{C}}_{j\ell}(r) = \{\psi^{*}_{j\ell}(r) + \psi_{j\ell}(r)\}/2,$$

$$\phi^{\mathrm{S}}_{j\ell}(r) = \{\psi^{*}_{j\ell}(r) - \psi_{j\ell}(r)\}/(2i), \quad (23)$$

with

$$\psi_{j\ell}(r) = r^{\ell}\exp[-\eta_j r^2], \quad \eta_j = (1+ib)/a_j^2, \quad (24)$$

i.e., Gaussian functions with a complex-range parameter. We thus refer to the basis $\phi^{\mathrm{C}}_{j\ell}$ and $\phi^{\mathrm{S}}_{j\ell}$ as the complex-range Gaussian basis.

The complex-range Gaussian basis functions are oscillating with r. They are therefore expected to simulate the oscillating pattern of the continuous breakup state wave functions better than the real-range Gaussian basis functions do. Moreover, numerical calculation with the complex-range Gaussians can be done using essentially the same computer programs as for the real-range Gaussians, just replacing real variables for a_j of Eq. (21) by complex ones. Usefulness of the real- and complex-range Gaussian basis functions in few-body calculations are extensively presented in the review work [20]. We here emphasize that even in the case where the projectile is assumed to be three-body system, the Gaussian basis functions are easily utilized in the CDCC calculation with the PS method. We return this point in Sec. V.

IV. NUMERICAL TEST OF THE PSEUDOSTATE METHOD

In the previous stringent test of CDCC with the Av and Mid methods [3,13], calculated elastic and breakup S-matrix elements were found to converge, for sufficiently large model space. In this section, we test the PS method by comparing the calculated S-matrix elements with those obtained with the Av method that converged within the error of 1% and hence forth called "exact" S-matrix elements. The test is made for two systems, $d+^{58}$Ni scattering at 80 MeV and ^{6}Li$+^{40}$Ca scattering at 156 MeV.

A. $d+^{58}$Ni scattering at 80 MeV

As for the orbital angular momentum of the projectile (d), we take $\ell=0$ and 2. It should be noted that the p-wave ($\ell=1$) breakup is negligible, because couplings $V_{\gamma\gamma'}(R)$ between odd and even parity breakup states contain contribution from $U_{\mathrm{pA}}(\mathbf{r}_{\mathrm{pA}})$ and $U_{\mathrm{nA}}(\mathbf{r}_{\mathrm{nA}})$ in opposite sign in Eq. (8). Table I shows the parameters of the potentials used; the interaction between a nucleon and the target is the nucleon-nucleus optical potential of Becchetti and Greenlees [21] at half the deuteron incident energy. The interaction between proton and neutron is a one-range Gaussian potential, $v_{np}=v_0\exp[-(r/r_0)^2]$ with $v_0=-72.15$ MeV and $r_0=1.484$ fm, which reproduces the radius and the binding energy of deuteron.

In the Av method the weight function is taken as $f_{i\ell}(k)=1$, since the projectile (deuteron) has no resonance state. The model space that gives convergence within error of 1% turns out to be $\Delta_{i\ell}=1.3/30$ fm^{-1} and $k_{\max}=1.3$ fm^{-1}. The resulting values of $k_{\max}$ and $\Delta_{i\ell}$ are different from those used in the previous analysis [13]; the main purpose of Ref. [13] was to show that the convergence of the CDCC solution was obtained within a model space of practical use and that the converged solution satisfied an appropriate boundary condition. The model space taken there, $k_{\max}=1.0$ fm^{-1} and $\Delta_{i\ell}=1/8$ fm^{-1}, is indeed enough for the elastic S-matrix elements and the dominant part of the breakup ones with the smaller k, therefore the elastic cross sections and the total breakup cross sections are well reproduced. However, the model space is found to be insufficient to obtain the "exact" S-matrix elements in the high-k region around 1.0 fm^{-1}, hence we take here $k_{\max}=1.3$ fm^{-1} and $\Delta_{i\ell}=1.3/30$ fm^{-1} as mentioned above.

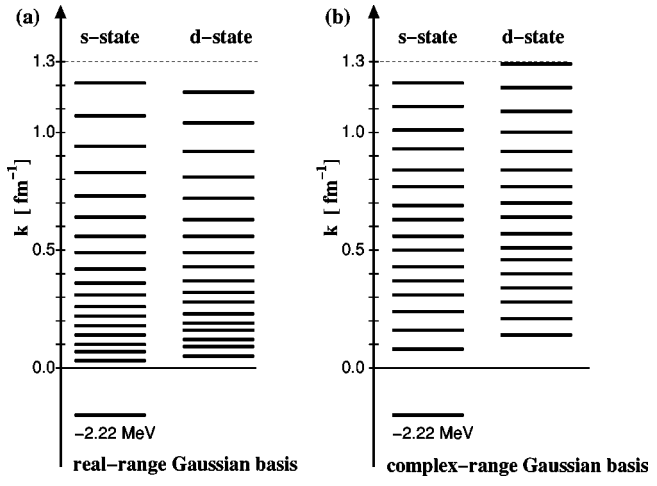

FIG. 3. Discretized momenta for real-range (a) and complex-range (b) Gaussian bases for deuteron. In each panel, the left (right) side corresponds to the s state (d state). The horizontal dotted line represents the cutoff momentum k_{cut} taken to be 1.3 fm^{-1}.

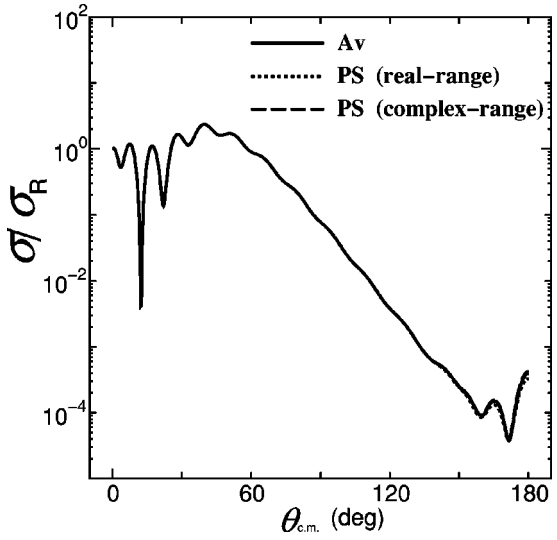

FIG. 4. Angular distribution of the elastic differential cross section as a ratio to the Rutherford one for $d+^{58}$Ni scattering at 80 MeV. Results with the Av method, and the real- and complex-range Gaussian PS methods are represented by the solid, dotted, and dashed lines, respectively.

In the real-range Gaussian PS method, a similar convergence is found, when the number of breakup channels, $N_{\rm PS}$, is 18 for both *s* and *d* waves. The number is even smaller when the complex-range Gaussian basis is taken: $N_{\rm PS}$ is 16 for *s* wave and 17 for *d* wave. The basis functions finally obtained have parameter sets $(a_1=1.0, a_n=30.0, n=30)$ for real-range Gaussian basis and $(a_1=1.0, a_n=20.0, 2n=40, b=\pi/2)$ for complex-range one. For both of them $N_{\rm PS}$ is smaller than the number of basis functions. High-lying states with $k>k_{\rm cut}=1.3$ fm^{-1}, which are obtained by diagonalizing $H_{\rm bc}$, do not affect the breakup *S*-matrix elements with $k \leqslant k_{\rm cut}$, because the coupling potentials between the two *k* regions are weak.

Figure 3 shows the discrete momenta $\hat{k}_{i\ell}$ translated from the eigenenergies $\epsilon_{i\ell}$ for the real- and complex-range Gaussian bases. One sees that for the real-range Gaussian basis, the discrete momenta are dense in the smaller *k* region and sparse in the larger *k* one. This distribution is not so effective in simulating the *k* continuum, in the higher *k* region in particular. For the complex-range Gaussian basis, on the other hand, the discrete momenta are distributed almost evenly. A similar sequence of the $\hat{k}_i$ is also seen for the case of the transformed harmonic oscillator basis of Ref. [16,22]. Such a sequence of $\hat{k}_i$ is close to that in the Av method. Thus, the complex-range Gaussian basis, as well as the transformed harmonic oscillator, is well suited for simulating the *k* continuum in the entire region $0<k\leqslant k_{\rm cut}$.

For the elastic *S*-matrix elements, both the real- and complex-range Gaussian PS methods well reproduce the "exact" one calculated with the Av method, as confirmed in Fig. 4 for the differential cross section. The three types of calculations, the real-range Gaussian PS (dotted line), the complex-range Gaussian PS (dashed line), and the Av methods (solid line), yield an identical cross section at all scattering angles. Thus, both of the PS methods proposed here are useful for treating the breakup effects on the elastic scattering.

Figure 5 shows the result for breakup *S*-matrix elements at the grazing total angular momentum $J=17$, as a function of *k*. The real-range Gaussian PS method (dashed line) well simulates the exact solution calculated with the Av method

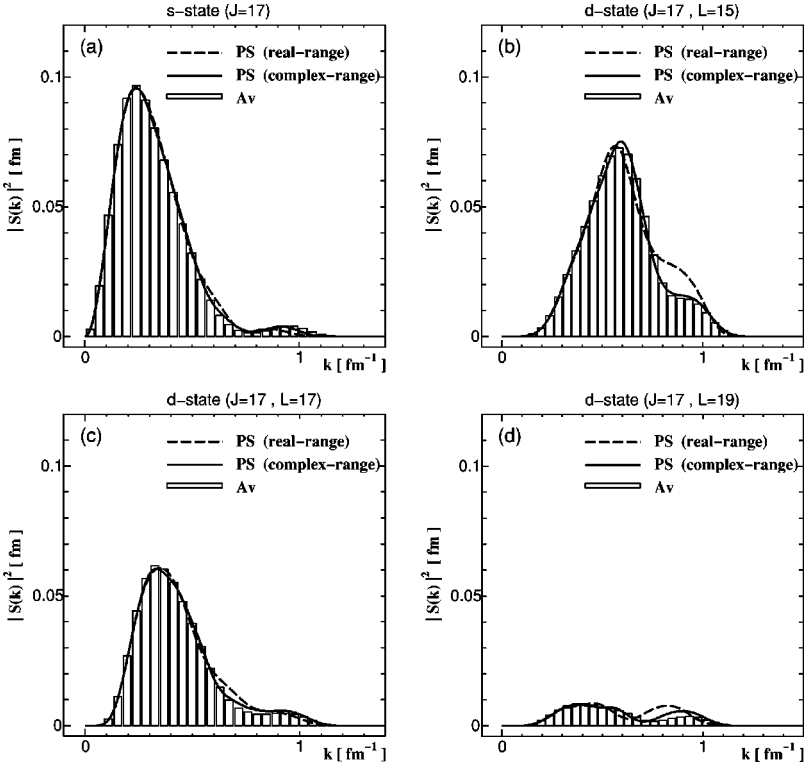

FIG. 5. The squared moduli of breakup *S*-matrix elements as a function of *k* at the grazing total angular momentum $J=17$ for $d+^{58}$Ni scattering at 80 MeV. The left upper panel (a) shows the result for the *s* state $(\ell=0, L=17)$. Results for the *d* state $(\ell=2)$ with $L=15$, 17, and 19 are, respectively, shown in (b), (c), and (d). In each panel, the dashed (solid) line represents the result of the real-range (complex-range) Gaussian PS method. The step line is the result for the "exact" *S*-matrix element calculated by the Av method.

TABLE II. The same as in Table I but for α+^{40}Ca at 104 MeV and d+^{58}Ca at 56 MeV.

System	V_0 (MeV)	r_0 (fm)	a_0 (fm)	W_0 (MeV)	r_W (fm)	a_W (fm)	W_D (MeV)	r_{WD} (fm)	a_{WD} (fm)
α+^{40}Ca	219.30	1.21	0.713	98.8	1.40	0.544			
d+^{58}Ca	75.470	1.20	0.769	2.452	1.32	0.783	9.775	1.32	0.783

(step line) in the lower k region that corresponds to the main components of the breakup S-matrix elements, but inaccurate in the higher k region around k=0.8 fm^{-1}. The deviation at higher k stems from the fact that real-range Gaussian basis poorly reproduces the continuum breakup state $\Phi_\ell(k,r)$ at the higher k. Figure 5 shows that this problem can be solved by using the complex-range Gaussian basis (solid line) instead.

B. ^{6}Li+^{40}Ca scattering at 156 MeV

Characteristic to this scattering, the projectile ^{6}Li has d-wave triplet resonance states (3^+, 2^+, 1^+). For simplicity, we neglect the intrinsic spin of ^{6}Li, following Refs. [1,5,6]. Then the projectile has only one d-wave resonance state with $\epsilon_{\rm res}$ =2.96 MeV and Γ=0.62 MeV. Obviously the energy and the width do not reproduce experimental data, but at least the elastic cross section of ^{6}Li is not affected much by the neglect of the spin [23].

In this scattering, the three-body system consists of deuteron, α, and ^{40}Ca. The interactions between each pair of the constituents are the optical potential of α+^{40}Ca scattering at 104 MeV [24], that of d+^{40}Ca scattering at 56 MeV [25], and $v_{\alpha d}=v_0\exp[-(r/r_0)^2]$ with v_0=−74.19 MeV and r_0 =2.236 fm. Table II shows the parameters of the optical potentials.

The model space sufficient for describing breakup processes in this scattering is $k_{\rm max}$=2.0 fm^{-1} and $\ell_{\rm max}$=2; the model space is composed of two k-continua for ℓ=0 and 2. Since there exists a resonance in ℓ=2, the d-wave k-continuum is further divided in the Av method into the resonant part [$0<k<0.55$] and the nonresonant part [$0.55<k<2.0$]. In the former region the k continuum of $\Phi_{i,\ell=2}(k,r)$ varies rapidly with k. The Av method can simulate this rapid change by taking $f_{i,\ell=2}(k)$=1 with bins of an extremely small width. In fact, clear convergence is found for both the elastic and the breakup S-matrix elements, when the resonance part is described by 30 bins and the nonresonance part of the d-wave and the s-wave k-continua by 20 bins. Another Av discretization, which has been widely used as a convenient prescription [1,5,6,8,10], is also made for comparison, in which the resonance region is represented by a single state with the weight factor of Breit-Wigner type given by Eq. (12). The two sorts of Av discretization are compared with the real- and complex-range Gaussian PS methods. With the PS methods, convergence of the S-matrix elements is found with 21 s-wave breakup channels and 22 d-wave ones. The level sequences of the resulting discrete eigenstates are shown in Fig. 6 for both the basis functions, which have the same properties as in Fig. 3. The parameter sets of the basis functions, finally taken in the PS methods, are (a_1 =1.0, a_n=30.0, n=30) for the real-range Gaussian basis and

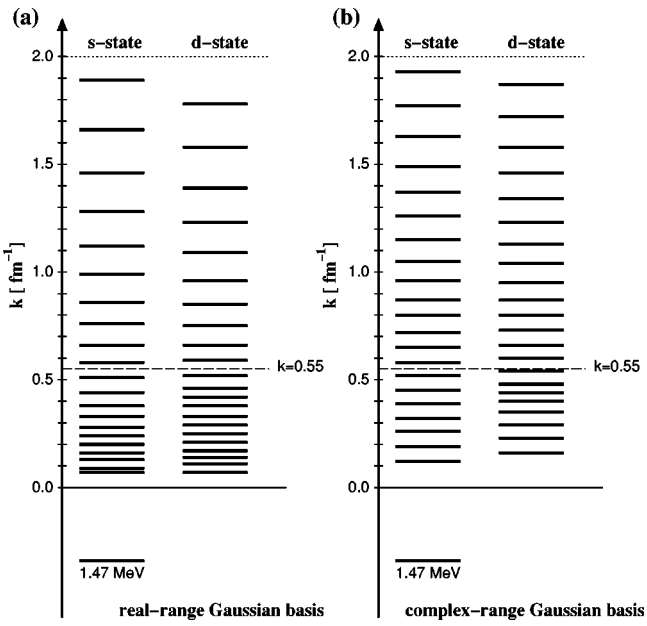

FIG. 6. The same as in Fig. 4 but for ^{6}Li; $k_{\rm cut}$ is taken to be 2.0 fm^{-1}. The horizontal dashed line corresponds to the border momentum between the resonance and nonresonance parts used in the Av method.

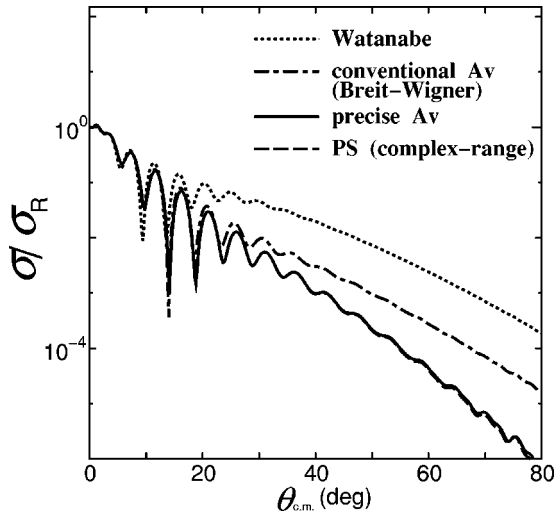

FIG. 7. Angular distribution of the elastic differential cross section (Rutherford ratio) for ^{6}Li+^{40}Ca scattering at 156 MeV. The results of the complex-range Gaussian PS method and the approximate treatment of the resonance of ^{6}Li, i.e., the conventional Av method with the weight factor of Breit-Wigner type, are shown by the dashed and dash-dotted lines, respectively. The solid line is the exact solution calculated by the Av method with dense bins and the dotted line is the result of Watanabe model, i.e., without breakup effects.

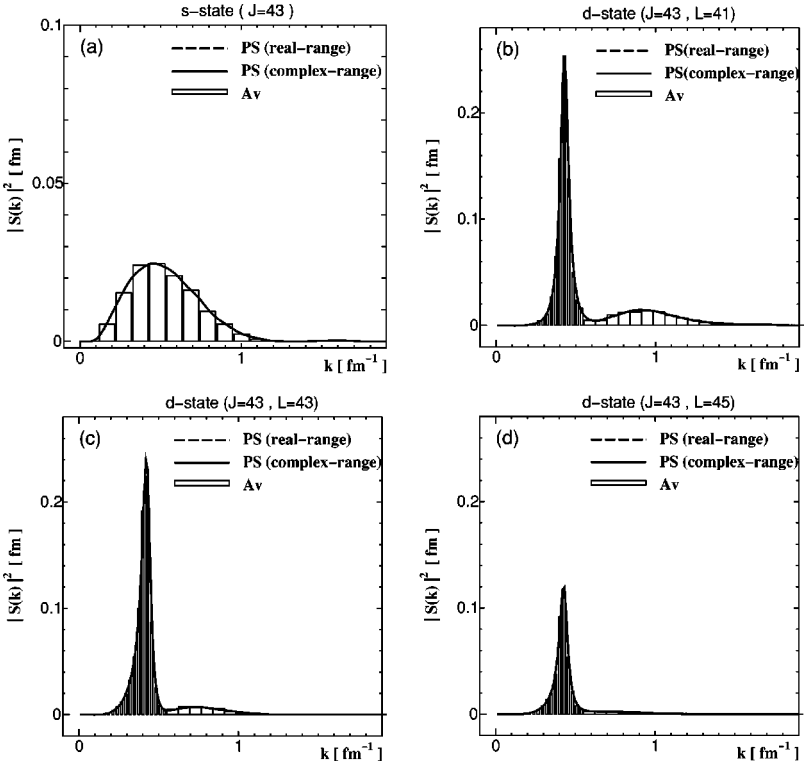

FIG. 8. The same as in Fig. 5 but for ^{6}Li $+^{40}$Ca scattering at 156 MeV. The corresponding grazing total angular momentum is 43. The step line is the result of the Av method with dense bins. Note that the difference between the results of the real- and complex-range Gaussian PS methods is not visible since it is less than about 1%.

(a_1=1.0, a_n=20.0, $2n$=40, $b=\pi/2$) for the complex-range one. For both bases $k_{\rm cut}$ is taken to be 2.0 fm^{-1}.

Figure 7 shows the differential cross section of the elastic scattering. The result with the precise Av discretization based on dense bins, considered to be the exact solution, is denoted by the solid line. The dotted line represents the result of the Watanabe model, i.e., with no breakup channels. The conventional Av discretization, based on the weight factor of Breit-Wigner type (dash-dotted line), well describes the breakup effects, particularly at forward angles ($\theta<20°$), but deviates considerably from the exact solution at larger angles ($\theta>30°$). The complex-range Gaussian PS discretization (dashed line) well reproduces the exact solution with a number of channels being suitable for practical use. The real-range Gaussian PS method gives just the same result as the complex-range one.

Figure 8 represents breakup S-matrix elements at grazing total angular momentum J=43. The real- and complex-range Gaussian PS discretization well reproduces the exact solution calculated by the Av discretization with dense bins. The results of the two PS methods turn out to coincide within the thickness of the line. The resonance peak can be expressed by only 8 (12) breakup channels in the complex-range (real-range) Gaussian PS method, while the corresponding number of breakup channels is 30 in the Av method, as mentioned above. Thus, one can conclude that the real- and complex-range Gaussian PS methods are very useful for describing not only nonresonant states but also resonant ones.

V. DISCUSSIONS ON FOUR-BODY BREAKUP REACTION

In the past CDCC calculations the projectile was assumed to be a two-body system, dealing only with three-body breakup reactions. In this section, we investigate the applicability of CDCC to four-body breakup reactions of the projectile consisting of three particles, $b+c+x$ (Fig. 9). The Av method needs the exact three-body wave functions being impossible to obtain. We can circumvent this problem with the present PS method; one can prepare an approximate complete set $\{\hat{\Phi}_{i\ell}\}$ by diagonalizing the Hamiltonian of the projectile in a space spanned by a set of basis functions of L^2 type. With $\{\hat{\Phi}_{i\ell}\}$ as the wave functions of the breakup channels, one can obtain an approximate total wave function $\Psi^{\rm CDCC}$ by solving CDCC equations (7). Inserting $\Psi^{\rm CDCC}$ into the exact form of breakup T-matrix elements in place of the exact total wave function, one reaches an approximate form:

$$T_4 = \langle e^{i(\mathbf{P}\cdot\mathbf{R}+\mathbf{k}\cdot\mathbf{r}+\mathbf{q}\cdot\mathbf{y})} | U_4 | \Psi^{\rm CDCC} \rangle_{\mathbf{R},\mathbf{r},\mathbf{y}}, \tag{25}$$

where U_4 is the sum of all interactions in the four-body system ($A+b+c+x$), $\mathbf{r}$ and $\mathbf{y}$ are two Jacobi coordinates of the three-body ($b+c+x$) system, and $\mathbf{k}(\mathbf{q})$ is the momentum being conjugate to $\mathbf{r}(\mathbf{y})$. The accuracy of Eq. (25)

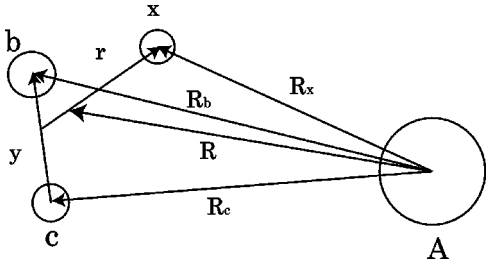

FIG. 9. Illustration of a four-body ($A+b+c+x$) system. The projectile consists of b, c, and x, and A is the target.

depends on how complete the set $\hat{\Phi}_{i\ell}$ is within the region $(0 \leqslant r \leqslant r_{\max}, 0 \leqslant y \leqslant y_{\max}, 0 \leqslant k \leqslant k_{\max}, 0 \leqslant q \leqslant q_{\max})$ being important for the breakup process considered. An important advantage of the use of the real- and complex-range Gaussian bases is that analytic integrations over **r** and **y** can be done in Eq. (25), by expanding U_4 in terms of a finite number of Gaussian basis functions. This makes the derivation of T_4 feasible. Analyses based on this formulation are of much interest as a future work.

VI. SUMMARY

The method of continuum discretized coupled channels (CDCC) is an accurate method of treating three-body breakup processes, in which the discretization of the *k* continuum is essential. In this paper, we proposed the new method of pseudostate (PS) discretization which can be used not only for virtual breakup processes in elastic scattering but also for breakup reactions. First we showed that an accurate transformation from the discrete breakup *S*-matrix elements calculated with the PS method to smooth ones is possible, since the PS basis functions can form in the good approximation a complete set in the finite region of **r** and **k** being important for the breakup processes. As bases satisfying the approximate completeness, we proposed to employ the real- and complex-range Gaussian bases; both of them can treat virtual breakup processes in the elastic scattering with high accuracy, i.e., with the error of calculated cross sections less than 1%. For breakup processes, the complex-range Gaussian basis is accurate throughout the entire region of the *k*-continuum concerned. The real-range Gaussian basis also keeps a good accuracy for the dominant part of breakup *S*-matrix elements with the lower *k*, although it is partially inaccurate for the higher *k* region. Thus, both bases can be used for realistic analyses of elastic scattering and projectile-breakup reactions including coincidence cross sections and energy spectra of ejected fragments.

The present new PS method has at least two advantages over the widely used momentum-bin average method. One is that it does not need the exact wave function of the projectile over the entire region of *r*. This is important from a theoretical point of view. The other is that with the real- and complex-range Gaussian bases one can calculate all the coupling potentials semianalytically [20], which is very useful in actual calculations. Furthermore, if the projectile has resonances in its excitation spectrum, the new method discretizes the complicated spectrum with a reasonable number of the basis functions, without distinguishing the resonance states from nonresonant continuous states. These advantages of the new method are extremely helpful, sometimes even essential, in applying CDCC to four-body breakup effects of unstable nuclei such as ^{6}He and ^{11}Li. The use of the Gaussian bases is promising for describing pseudobreakup states of these projectiles consisting of three fragments (core+n+n) [20]. Actually, a CDCC study of four-body breakup effects on the ^{6}He elastic scattering from ^{12}C at 38.3 MeV/nucleon is in progress [26], and the result of the analysis will be reported in a forthcoming paper.

ACKNOWLEDGMENTS

The authors would like to thank M. Kawai for helpful discussions. This work has been supported in part by the Grants-in-Aid for Scientific Research (Grant Nos. 12047233, and 14540271) of Monbukagakusyou of Japan.

[1] M. Kamimura, M. Yahiro, Y. Iseri, Y. Sakuragi, H. Kameyama, and M. Kawai, Prog. Theor. Phys. Suppl. **89**, 1 (1986).
[2] N. Austern, Y. Iseri, M. Kamimura, M. Kawai, G. H. Rawitscher, and M. Yahiro, Phys. Rep. **154**, 125 (1987).
[3] M. Yahiro, N. Nakano, Y. Iseri, and M. Kamimura, Prog. Theor. Phys. **67**, 1467 (1982).
[4] M. Yahiro, Y. Iseri, M. Kamimura, and M. Nakano, Phys. Lett. **141B**, 19 (1984).
[5] Y. Sakuragi and M. Kamimura, Phys. Lett. **149B**, 307 (1984).
[6] Y. Sakuragi, Phys. Rev. C **35**, 2161 (1987).
[7] Y. Sakuragi, M. Kamimura, and K. Katori, Phys. Lett. B **205**, 204 (1988).
[8] Y. Sakuragi, M. Yahiro, M. Kamimura, and M. Tanifuji, Nucl. Phys. **A480**, 361 (1988).
[9] Y. Iseri, H. Kameyama, M. Kamimura, M. Yahiro, and M. Tanifuji, Nucl. Phys. **A490**, 383 (1988).
[10] Y. Hirabayashi and Y. Sakuragi, Phys. Rev. Lett. **69**, 1892 (1992).
[11] J. A. Tostevin, D. Bazin, B. A. Brown, T. Glasmacher, P. G. Hansen, V. Maddalena, A. Navin, and B. M. Sherrill, Phys. Rev. C **66**, 024607 (2002); A. M. Moro, R. Crespo, F. Nunes, and I. J. Thompson, *ibid.* **66**, 024612 (2002), and references therein.
[12] K. Ogata, M. Yahiro, Y. Iseri, and M. Kamimura, Phys. Rev. C **67**, R011602 (2003).
[13] R. A. D. Piyadasa, M. Kawai, M. Kamimura, and M. Yahiro, Phys. Rev. C **60**, 044611 (1999).
[14] N. Austern, M. Yahiro, and M. Kawai, Phys. Rev. Lett. **63**, 2649 (1989); N. Austern, M. Kawai, and M. Yahiro, Phys. Rev. C **53**, 314 (1996).
[15] M. Yahiro and M. Kamimura, Prog. Theor. Phys. **65**, 2046 (1981); **65**, 2051 (1981).
[16] A. M. Moro, J. M. Arias, J. Gómez-Camacho, I. Martel, F. Pérez-Bernal, R. Crespo, and F. Nunes, Phys. Rev. C **65**, 011602 (2002).
[17] R. Y. Rasoanaivo and G. H. Rawitscher, Phys. Rev. C **39**, 1709 (1989).
[18] J. A. Tostevin, F. M. Nunes, and I. J. Thompson, Phys. Rev. C **63**, 024617 (2001).
[19] M. Kamimura, Phys. Rev. A **38**, 621 (1988).
[20] E. Hiyama, Y. Kino, and M. Kamimura, Prog. Part. Nucl. Phys. **51**, 223 (2003).

[21] F. D. Becchetti, Jr. and G. W. Greenlees, Phys. Rev. **182**, 1190 (1969).
[22] F. Pérez-Bernal, I. Martel, J. M. Arias, and J. Gómez-Camacho, Phys. Rev. A **63**, 052111 (2001).
[23] H. Ohnishi, M. Tanifuji, M. Kamimura, Y. Sakuragi, and M. Yahiro, Nucl. Phys. **A415**, 271 (1984).
[24] G. Hauser, R. Löhken, G. Nowicki, H. Rebel, G. Schatz, G. Schweimer, and J. Specht, Nucl. Phys. **A182**, 1 (1972).
[25] N. Matsuoka, H. Sakai, T. Saito, K. Hosono, M. Kondo, H. Ito, K. Hatanaka, T. Ichihara, A. Okihana, K. Imai, and K. Nisimura, Nucl. Phys. **A455**, 413 (1986).
[26] T. Matsumoto, E. Hiyama, K. Ogata, M. Yahiro, Y. Iseri, and M. Kamimura, a talk at the Third Conference on Direct Reactions with Exotic Beams, Surrey, July 10–12, 2003 (unpublished).